DE GRUYTER OPEN
DOI: 10.1515/ace-2015-0069
ARCHIVES OF CIVIL ENGINEERING
Vol. LXII ISSUE 2 2016

THREE-POINT BENDING OF SEVEN LAYER BEAMS – – THEORETICAL AND EXPERIMENTAL STUDIES

E. MAGNUCKA-BLANDZI[1], P. PACZOS[2], P. WASILEWICZ[3], A.WYPYCH[4]

The subject of the analytical and experimental studies therein is of two metal seven-layer beam – plate bands. The first beam – plate band is composed of a lengthwise trapezoidally corrugated main core and two crosswise trapezoidally corrugated cores of faces. The second beam – plate band is composed of a crosswise trapezoidally corrugated main core and two lengthwise trapezoidally corrugated cores of faces. The hypotheses of deformation of a normal to the middle surface of the beams after bending are formulated. Equations of equilibrium are derived based on the theorem of minimum total potential energy. Three-point bending of the simply supported beams is theoretically and experimentally studied. The deflections of the two beams are determined with two methods, compared and presented.

Keywords: trapezoidally corrugated cores, orthotropic structures, layered plate-bands

1. INTRODUCTION

Layered structures have been the subject of study since the mid-twentieth century. Carrera and Brischetto [1] and Vinson [11] presented problems of modelling and calculation of the sandwich structures. Cheon and Kim [2] formulated an equivalent plate model for the corrugated core of sandwich panels. Kazemahvazi and Zenkert [3] developed an analytical model of corrugated

[1] DSc., PhD., Eng., Poznan University of Technology, Institute of Mathematics, ul. Piotrowo 3A, 60-965 Poznań, Poland, e-mail: ewa.magnucka-blandzi@put.poznan.pl
[2] DSc., PhD., Eng., Poznan University of Technology, Institute of Applied Mechanics, ul. Jana Pawła II 24, 60-965 Poznań, Poland, e-mail: piotr.paczos@put.poznan.pl
[3] PhD., Eng., Poznan University of Technology, Institute of Applied Mechanics, ul. Jana Pawła II 24, 60-965 Poznań, Poland, e-mail: piotr.wasilewicz@put.poznan.pl
[4] PhD., Eng., Poznan University of Technology, Institute of Materials Science and Engineering, ul. Jana Pawła II 24, 60-965 Poznań, Poland, e-mail: artur.wypych@put.poznan.pl

composite cores. Kotełko et al [4] presented the problem of estimating the load-carrying capacity of multi-layer plated structures. Lewiński et al [5], Magnucka-Blandzi and Magnucki [6] presented a theoretical study of transverse shear modulus of elasticity for thin-walled corrugated cores of sandwich beams. Magnucka-Blandzi et al [7] presented a mathematical modelling of the shearing effect for sandwich beams with sinusoidal corrugated cores. Magnucki et al [8] described theoretical studies of elastic bending and buckling of a steel seven-layer beam with a corrugated main core and sandwich faces. Paczos et al [9] presented theoretical and experimental studies of five-layer beams. Seong et al [10] described the bending problem of sandwich plates with bi-directional corrugated cores. Piekarczyk and Grec [12] described achievements in gluing technique in steel and aluminium structures. Design rules of adhesive connections and basic methods for their calculations are mentioned. The most significant examples of the applications of those joints in steel as well as aluminium structures are presented. Another approach was presented by Książek et al. [13] who concentrated on objective decisions in the construction. The authors presented a comparison of different methods used for multi-criteria decision-making.

2. ANALYTICAL MODELLING OF SEVEN-LAYER BEAMS

2.1. THE FIRST BEAM – PLATE BAND

The first beam – plate band (B-1) with a lengthwise trapezoidally corrugated main core and two crosswise trapezoidally corrugated cores of faces is shown in Fig. 1. The direction of the corrugation of the main core and the face cores are orthogonal. The beam measurements are as follows: L – length, b – width, t_{c1} – depth of the main core, t_{c2} – depth of facing cores, t_s – thicknesses of flat sheets.

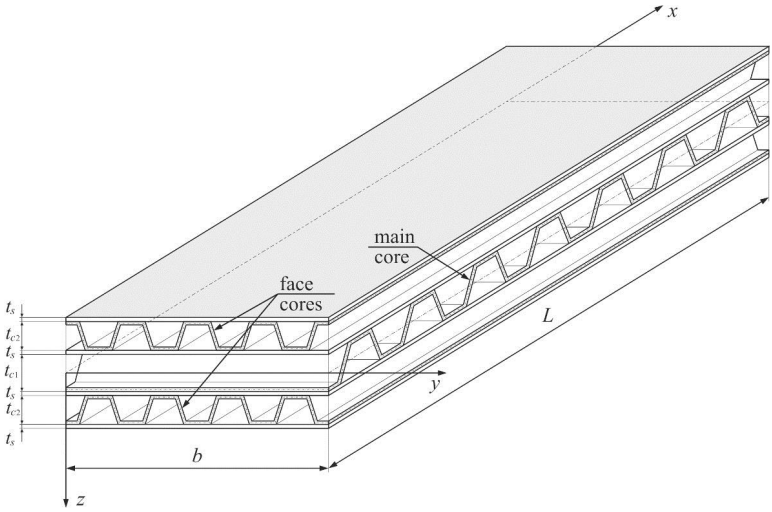

Fig. 1. Scheme of the first beam – plate band (B-1)

The sizes of the trapezoidal corrugations of the main core and facing cores are shown in Fig. 2. The index i=1 refers to the main core, while the index i=2 refers to the face cores. The length of one pitch of the corrugation is b_{0i}, the base of the trapezoid is b_{fi}, and thickness of the corrugated sheet is t_{0i}.

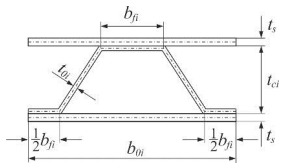

Fig. 2. Scheme of trapezoidal corrugations of the main core (i=1) or face cores (i=2)

The analytical model of the beam is formulated with regard to the broken line hypothesis (Fig. 3). This hypothesis for multi-layer structures is described in detail by Magnucka-Blandzi et al [7] and Magnucki et al [8].

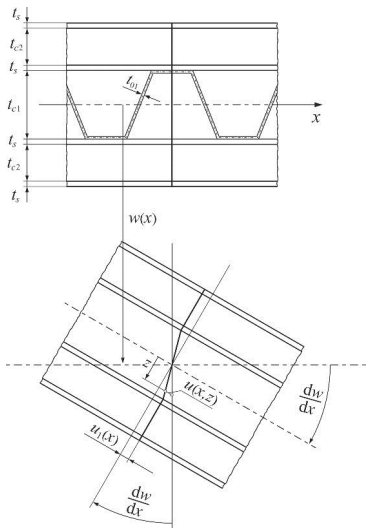

Fig. 3. Scheme of the deformation of a plane cross-section of the seven-layer beam (B-1)

Displacements with consideration of this hypothesis are as follows:

- the upper sandwich facing

$$u(x,z) = -t_{c1}\left[\zeta \frac{dw}{dx} + \psi(x)\right], \text{ for } -\left(\frac{1}{2} + 2x_1 + x_2\right) \le \zeta \le -\frac{1}{2}, \tag{2.1}$$

- the main corrugated core

$$u(x,z) = -t_{c1}\zeta\left[\frac{dw}{dx} - 2\psi(x)\right], \text{ for } -\frac{1}{2} \le \zeta \le \frac{1}{2}, \tag{2.2}$$

- the lower sandwich facing

$$u(x,z) = -t_{c1}\left[\zeta \frac{dw}{dx} + \psi(x)\right], \text{ for } \frac{1}{2} \le \zeta \le \frac{1}{2} + 2x_1 + x_2, \tag{2.3}$$

where:

$x_1=t_s/t_{c1}$, $x_2=t_{c2}/t_{c1}$ – dimensionless parameters, $\zeta=z/t_{c1}$ – dimensionless coordinate, $\psi(x)=u_1(x)/t_{c1}$ – dimensionless displacements, $u_1(x)$ – displacements in the x direction and $w(x)$ – deflection (Fig. 3).

Thus, the strains are as follows:

- the upper (the sign "+")/lower (the sign "-") sandwich facing

$$\varepsilon_x = \frac{\partial u}{\partial x} = -t_{c1}\left(\zeta \frac{d^2 w}{dx^2} \pm \frac{d\psi}{dx}\right), \text{ and } \gamma_{xz} = \frac{\partial u}{\partial z} + \frac{dw}{dx} = 0, \tag{2.4}$$

- the main corrugated core

$$\varepsilon_x = \frac{\partial u}{\partial x} = -t_{c1}\zeta\left(\frac{d^2 w}{dx^2} - 2\frac{d\psi}{dx}\right), \text{ and } \gamma_{xz} = \frac{\partial u}{\partial z} + \frac{dw}{dx} = 2\psi(x). \tag{2.5}$$

The elastic strain energy of the beam – plate band (B-1) is a sum of the energy of particular layers

$$U_{\varepsilon}^{(B-1)} = U_{\varepsilon}^{(c-1)} + U_{\varepsilon}^{(s-i)} + U_{\varepsilon}^{(c-2)} + U_{\varepsilon}^{(s-o)}, \tag{2.6}$$

where:

- the energy of the main corrugated core

$$U_{\varepsilon}^{(c-1)} = E_s b t_{c1}^3 \int_0^L \left\{ \frac{1}{24} \widetilde{E}_x^{(c-1)} \left[\left(\frac{d^2 w}{dx^2} \right)^2 - 4 \frac{d^2 w}{dx^2} \frac{d\psi}{dx} + 4 \left(\frac{d\psi}{dx} \right)^2 \right] + 2 \widetilde{G}_{xz}^{(c-1)} \left(\frac{\psi(x)}{t_{c1}} \right)^2 \right\} dx, \tag{2.7}$$

- the energy of the corrugated cores of facings

$$U_{\varepsilon}^{(c-2)} = E_s b t_{c1}^3 \frac{x_2 x_{02}}{x_{b2}} \int_0^L \left[C_{ww}^{(c-2)} \left(\frac{d^2 w}{dx^2} \right)^2 - C_{w\psi}^{(c-2)} \frac{d^2 w}{dx^2} \frac{d\psi}{dx} + C_{\psi\psi}^{(c-2)} \left(\frac{d\psi}{dx} \right)^2 \right] dx, \tag{2.8}$$

- the energy of the inner and outer sheets

$$U_{\varepsilon}^{(s)} = U_{\varepsilon}^{(s-i)} + U_{\varepsilon}^{(s-o)} = E_s b t_{c1}^3 \int_0^L \left[C_{ww}^{(s)} \left(\frac{d^2 w}{dx^2} \right)^2 - C_{w\psi}^{(s)} \frac{d^2 w}{dx^2} \frac{d\psi}{dx} + 2 x_1 \left(\frac{d\psi}{dx} \right)^2 \right] dx. \tag{2.9}$$

Thus, the elastic strain energy of the first seven-layer beam (2.6) is in the following form

$$U_{\varepsilon}^{(B-1)} = E_s b t_{c1}^3 \int_0^L \left[\frac{1}{2} C_{ww}^{(B-1)} \left(\frac{d^2 w}{dx^2} \right)^2 - C_{w\psi}^{(B-1)} \frac{d^2 w}{dx^2} \frac{d\psi}{dx} + \frac{1}{2} C_{\psi\psi}^{(B-1)} \left(\frac{d\psi}{dx} \right)^2 + 2 \widetilde{G}_{xz}^{(c-1)} \left(\frac{\psi(x)}{t_{c1}} \right)^2 \right] dx, \tag{2.10}$$

where:

$C_{ww}^{(B-1)}$, $C_{w\psi}^{(B-1)}$, $C_{\psi\psi}^{(B-1)}$ – dimensionless parameters of composite structures, $\widetilde{G}_{xz}^{(c-1)}$ – dimensionless shear modulus of elasticity of the main corrugated core [5], E_s – Young's modulus.

The work of the load

$$W = \int_0^L qw(x)dx\,, \tag{2.11}$$

where:

q – intensity of the transverse load.

The system of the equations of equilibrium – two differential equations derived based on the theorem of minimum potential energy $\delta\left(U_{\varepsilon}^{(B-1)} - W\right) = 0$, is in the following form

$$C_{ww}^{(B-1)}\frac{d^2w}{dx^2} - C_{w\psi}^{(B-1)}\frac{d\psi}{dx} = -\frac{M_b(x)}{E_s b t_{c1}^3} \quad \text{and} \quad C_{w\psi}^{(B-1)}\frac{d^3w}{dx^3} - C_{\psi\psi}^{(B-1)}\frac{d^2\psi}{dx^2} + 4\widetilde{G}_{xz}^{(c-1)}\frac{\psi(x)}{t_{c1}^2} = 0\,. \tag{2.12}$$

Three-point bending of the seven-layer beam – plate band (B-1) is shown in Fig. 4.

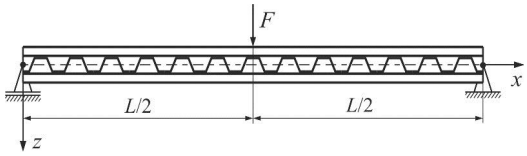

Fig. 4. Scheme of the three-point bending of the first beam (B-1)

The system of two differential equations (2.12) is reduced to one differential equation in the following form

$$\frac{d^2\psi}{dx^2} - \left(\frac{k}{t_{c1}}\right)^2 \psi(x) = -C_q \frac{Q(x)}{E_s b t_{c1}^3} \tag{2.13}$$

where:

$k = 2\sqrt{\dfrac{C_{ww}^{(B-1)}\widetilde{G}_{xz}^{(c-1)}}{C_{ww}^{(B-1)}C_{\psi\psi}^{(B-1)} - \left(C_{w\psi}^{(B-1)}\right)^2}}$, $C_q = \dfrac{C_{w\psi}^{(B-1)}}{C_{ww}^{(B-1)}C_{\psi\psi}^{(B-1)} - \left(C_{w\psi}^{(B-1)}\right)^2}$ – dimensionless parameters, $Q(x) = \dfrac{dM_b}{dx}$ – the shear force.

The general solution of the equation (2.13) is in the form

$$\psi(x) = C_1 \sinh\left(k\frac{x}{t_{c1}}\right) + C_2 \cosh\left(k\frac{x}{t_{c1}}\right) + \psi_p(x) \tag{2.14}$$

where:

C_1, C_2 – integration constants, $\psi_p = \dfrac{C_{w\psi}^{(B-1)}}{8C_{ww}^{(B-1)}\widetilde{G}_{xz}^{(c-1)}}\dfrac{F}{E_s b t_{c1}}$ – particular solution.

Taking into account the boundary conditions for the half beam $\left.\dfrac{d\psi}{dx}\right|_{x=0} = 0$ and $\psi\left(\dfrac{L}{2}\right) = 0$ the integration constants $C_1 = 0$ and $C_2 = -\cosh^{-1}\left(\dfrac{kL}{2t_{c1}}\right)\psi_0$ are determined. Then, the dimensionless displacement (2.14) is in the following form

$$\psi(x) = \left[1 - \cosh\left(k\frac{x}{t_{c1}}\right)\cosh^{-1}\left(\frac{kL}{2t_{c1}}\right)\right]\psi_p . \tag{2.15}$$

Substituting this function (2.15) and the bending moment $M_b(x) = Fx/2$ for $0 \le x \le L/2$ to the first equation (2.12), and taking into account the boundary conditions for the half beam $w(0) = 0$ and $dw/dx\big|_{x=L/2} = 0$, the maximum deflection is determined, i.e. the deflection in the middle span of the beam in the following form

$$w_{\max}^{(B-1)} = w\left(\frac{L}{2}\right) = \left\{1 + 3\left[1 - \frac{2t_{c1}}{kL}\tanh\left(\frac{kL}{2t_{c1}}\right)\right]\frac{\left(C_{w\psi}^{(B-1)}\right)^2}{C_{ww}^{(B-1)}\widetilde{G}_{xz}^{(c-1)}}\left(\frac{t_{c1}}{L}\right)^2\right\}\frac{F}{48C_{ww}^{(B-1)}E_s b}\left(\frac{L}{t_{c1}}\right)^3 . \tag{2.16}$$

2.2. THE SECOND BEAM – PLATE BAND

The second beam – plate band (B-2) with the crosswise trapezoidally corrugated main core and two lengthwise trapezoidally corrugated cores of faces is shown in Fig. 5. The direction of corrugation of the main core and the face cores are orthogonal. The sizes of the beam are analogous to the first beam.

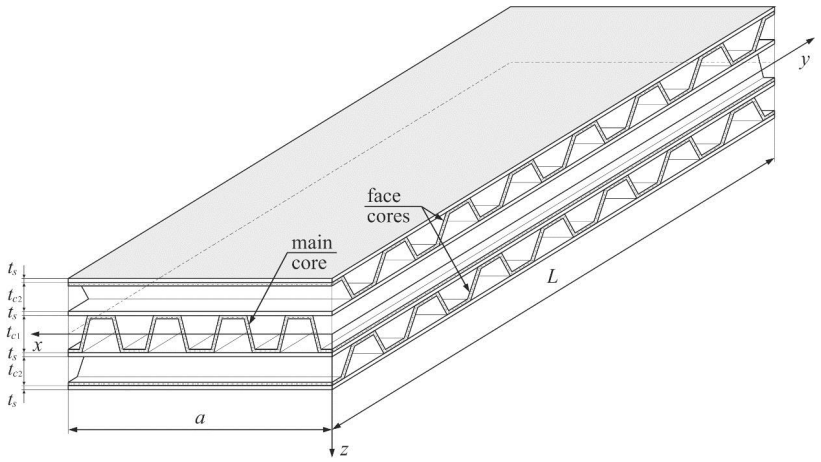

Fig. 5. Scheme of the second beam – plate band (B-2)

The analytical model of the beam is formulated with regard to the broken line hypothesis (Fig. 6). Displacements with consideration of this hypothesis are as follows:

- the upper sheet

$$v(y,z) = -t_{c1}\left[\zeta\frac{dw}{dy} + x_2\phi(y)\right], \text{ for } -\left(\frac{1}{2} + 2x_1 + x_2\right) \le \zeta \le -\left(\frac{1}{2} + x_1 + x_2\right), \tag{2.17}$$

- the upper core of the face

$$v(y,z) = -t_{c1}\left\{\zeta\frac{dw}{dy} - \left[\zeta + \left(\frac{1}{2} + x_1\right)\right]\phi(y)\right\}, \text{ for } -\left(\frac{1}{2} + x_1 + x_2\right) \le \zeta \le -\left(\frac{1}{2} + x_1\right), \tag{2.18}$$

- the main core with two inner sheets

$$v(y,z) = -t_{c1}\zeta\frac{dw}{dy}, \text{ for } -\left(\frac{1}{2} + x_1\right) \le \zeta \le \frac{1}{2} + x_1, \tag{2.19}$$

- the lower core of the face

$$v(y,z) = -t_{c1}\left\{\zeta\frac{dw}{dy} - \left[\zeta - \left(\frac{1}{2} + x_1\right)\right]\phi(y)\right\}, \text{ for } \frac{1}{2} + x_1 \le \zeta \le \frac{1}{2} + x_1 + x_2, \tag{2.20}$$

- the lower sheet

$$v(y,z) = -t_{c1}\left[\zeta\frac{dw}{dy} - x_2\phi(y)\right], \text{ for } \frac{1}{2} + x_1 + x_2 \le \zeta \le \frac{1}{2} + 2x_1 + x_2, \tag{2.21}$$

where:

$\phi(x)=v_1(y)/t_{c2}$ – dimensionless displacements, $v_1(y)$ – displacements in the y direction and $w(y)$ – deflection (Fig. 6).

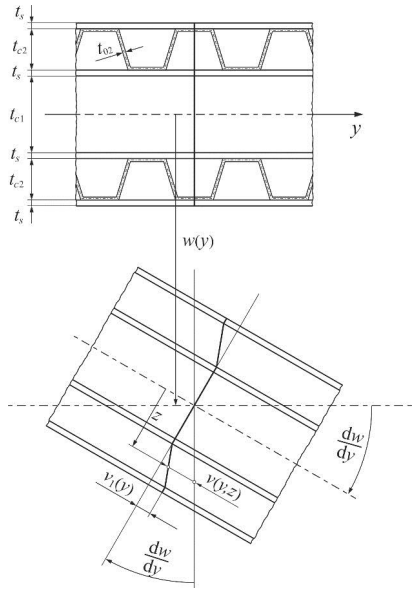

Fig. 6. Scheme of the deformation of a plane cross-section of the seven-layer beam (B-2)

Thus, the strains are as follows:

- the upper (the sign "+")/lower (the sign "– ") sheets

$$\varepsilon_y = \frac{\partial v}{\partial y} = -t_{c1}\left[\zeta \frac{d^2 w}{dy^2} \pm x_2 \frac{d\phi}{dy}\right], \text{ and } \gamma_{yz} = \frac{\partial v}{\partial z} + \frac{dw}{dy} = 0, \tag{2.22}$$

- the upper(the sign "+")/lower (the sign "– ") core of the face

$$\varepsilon_y = \frac{\partial v}{\partial y} = -t_{c1}\left\{\zeta \frac{d^2 w}{dy^2} - \left[\zeta \pm \left(\frac{1}{2} + x_1\right)\right]\frac{d\phi}{dy}\right\}, \text{ and } \gamma_{yz} = \frac{\partial v}{\partial z} + \frac{dw}{dy} = \phi(y), \tag{2.23}$$

- the main core with two inner sheets

$$\varepsilon_y = \frac{\partial v}{\partial y} = -t_{c1}\zeta \frac{d^2 w}{dy^2}, \text{ and } \gamma_{yz} = \frac{\partial v}{\partial z} + \frac{dw}{dy} = 0. \tag{2.24}$$

The elastic strain energy of the beam – plate band (B-2) is a sum of the energy of particular layers, the same as for the first beam (2.6), therefore, it takes the following form

$$U_{\varepsilon}^{(B-2)} = E_s a t_{c1}^3 \int_0^L \left[\frac{1}{2} C_{ww}^{(B-2)} \left(\frac{d^2 w}{dy^2}\right)^2 - C_{w\phi}^{(B-2)} \frac{d^2 w}{dy^2}\frac{d\phi}{dy} + C_{\psi\psi}^{(B-2)} \left(\frac{d\psi}{dy}\right)^2 + x_2 \widetilde{G}_{yz}^{(c-2)} \left(\frac{\psi(x)}{t_{c1}}\right)^2\right] dx, \tag{2.25}$$

where:

$C_{ww}^{(B-2)}, C_{w\psi}^{(B-2)}, C_{\psi\psi}^{(B-2)}$ – dimensionless parameters of composite structures, $\widetilde{G}_{xz}^{(c-2)}$ – dimensionless shear modulus of elasticity of the main corrugated core [5].

The system of the equations of equilibrium – two differential equations based on the theorem of minimum potential energy $\delta\left(U_{\varepsilon}^{(B-2)} - W\right) = 0$, are in the following forms

$$C_{ww}^{(B-2)} \frac{d^2 w}{dy^2} - C_{w\phi}^{(B-2)} \frac{d\phi}{dy} = -\frac{M_b(y)}{E_s a t_{c1}^3} \text{ and } C_{w\phi}^{(B-2)} \frac{d^3 w}{dy^3} - 2C_{\phi\phi}^{(B-2)} \frac{d^2 \phi}{dy^2} + 2x_2 \widetilde{G}_{yz}^{(c-2)} \frac{\psi(y)}{t_{c1}^2} = 0. \tag{2.26}$$

This system of the equations of equilibrium is analogically solved as for the first beam. Thus, for three-point bending of the seven-layer beam – plate band (B-2) shown in Fig. 7, the deflection in the middle span of the beam is in the following form

$$(2.27)\quad w_{\max}^{(B-2)} = w\left(\frac{L}{2}\right) = \left\{1+3\left[1-\frac{2t_{c1}}{kL}\tanh\left(\frac{kL}{2t_{c1}}\right)\right]\frac{\left(C_{w\phi}^{(B-2)}\right)^2}{C_{ww}^{(B-2)}x_2\widetilde{G}_{xz}^{(c-2)}}\left(\frac{t_{c1}}{L}\right)^2\right\}\frac{F}{48C_{ww}^{(B-2)}E_s a}\left(\frac{L}{t_{c1}}\right)^3.$$

where:

$k = \sqrt{\dfrac{2C_{ww}^{(B-2)}x_2\widetilde{G}_{yz}^{(c-2)}}{2C_{ww}^{(B-2)}C_{\phi\phi}^{(B-2)}-\left(C_{w\phi}^{(B-2)}\right)^2}}$ is dimensionless parameter.

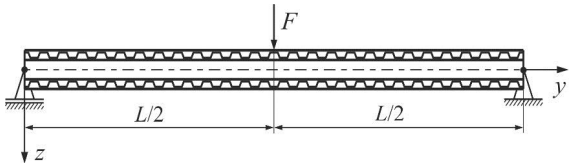

Fig. 7. Scheme of the three-point bending of the second beam (B-2)

3. EXPERIMENTAL TESTS OF THREE-POINT BENDING OF SEVEN-LAYER BEAMS

3.1. THE FIRST BEAM – PLATE BAND

The view of the first steel beam (B-1) located in the ZWICK test machine is shown in Fig. 8.

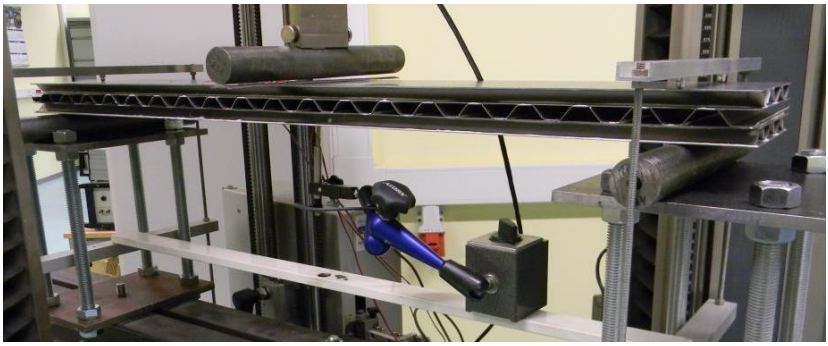

Fig. 8. The view of the first beam (B-1) located in the test machine

The scheme of the support of this beam in the test machine is shown in Fig. 9.

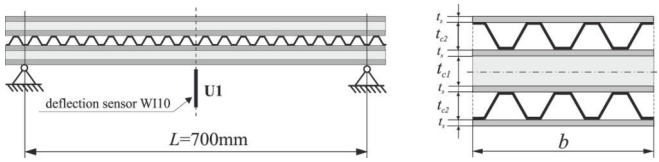

Fig. 9. The scheme of the support of the first beam (B-1) in the test machine

The sizes and Young's modulus of the first steel beam (B-1) are as follows: L=700 mm, b=120 mm, t_s=0.6 mm, t_{c1}=t_{c2}=11.0 mm, b_{01}=b_{02}=40.0 mm, b_{f1}=b_{f2}=10.0 mm, t_{01}=t_{02}=0.6 mm, E=2·10^5 MPa. Thus, the analytical linear dependence (2.16) between the deflection and the load-force for the three-point bending of this beam is in the form $w_{\max}^{(B-1)} = F / k_{B-1}^{(Analyt)}$, where the stiffness of the beam $k_{B-1}^{(Analyt)} = 1.862 \frac{\text{kN}}{\text{mm}}$. Hence, the load-force $F^{(Analyt)} = w_{\max}^{(B-1)} \cdot k_{B-1}^{(Analyt)}$.

The experimental dependence (the solid line) between the load-force and the deflection of the three-point bending of this beam is shown in Fig. 10. Additionally, the analytical linear dependence (the broken line) for this beam is presented with a view to compare both methods.

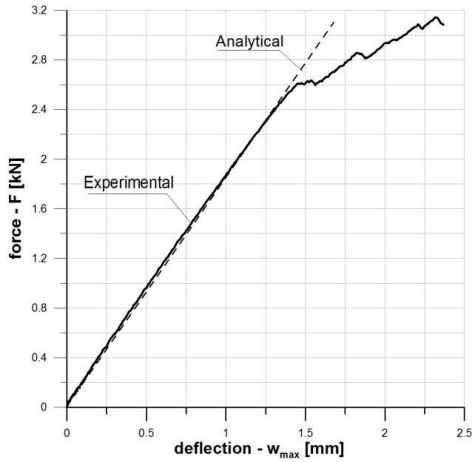

Fig. 10. The experimental and analytical force-deflection curves of the three-point bending (B-1)

The analytical solution for the first beam in the linear dependence form (the broken line) approaches the experimental curve (the solid line).

Example values of the analytical and experimental dependences $F(w_{\max})$ are specified in the Table 1.

Table 1. Example values of deflections and load-forces (Fig. 10)

$w_{\max}$ [mm]	0.25	0.50	0.75	1.00	1.152
$F^{(Exp)}$ [kN]	0.496	0.963	1.425	1.875	2.145
$F^{(Analyt)}$ [kN]	0.466	0.931	1.397	1.862	2.145

The relative difference between the analytical $F^{(Analyt)}$ and experimental $F^{(Exp)}$ values of load-forces is below 5%.

3.2. THE SECOND BEAM – PLATE BAND

The view of the second steel beam (B-2) located in the ZWICK test machine is shown in Fig. 11.

Fig. 11. The view of the second beam (B-2) located in the test machine

The scheme of the support of this beam in the test machine is shown in Fig. 12.

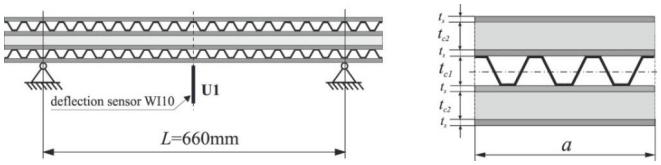

Fig. 12. The scheme of the support of the second beam (B-2) in the test machine

The sizes and Young's modulus of the second steel beam (B-2) are as follows: L=660 mm, a=120 mm, t_s=0.6 mm, $t_{c1}=t_{c2}$=11.0 mm, $b_{01}=b_{02}$=40.0 mm, $b_{f1}=b_{f2}$=10.0 mm, $t_{01}=t_{02}$=0.6 mm, E=2·10^5 MPa. Thus, the analytical linear dependence (2.27) between the deflection and the load-force of the three-point bending of this beam is in the form $w_{\max}^{(B-2)} = F \big/ k_{B-2}^{(Analyt)}$, where the stiffness of the beam $k_{B-2}^{(Analyt)} = 1.303 \dfrac{\text{kN}}{\text{mm}}$. Hence, the load-force $F^{(Analyt)} = w_{\max}^{(B-2)} \cdot k_{B-2}^{(Analyt)}$.

Example values of the analytical and experimental dependences $F(w_{\max})$ are specified in the Table 2.

Table 2. Example values of deflections and load-forces (Fig. 13)

$w_{\max}$ [mm]	1.00	1.25	1.50	1.75	2.00	2.421
$F^{(Exp)}$ [kN]	1.437	1.779	2.105	2.412	2.715	3.154
$F^{(Analyt)}$ [kN]	1.303	1.629	1.955	2.280	2.606	3.154

The relative difference between the analytical $F^{(Analyt)}$ and experimental $F^{(Exp)}$ values of load-forces for the second beam is below 10% and it exceeds the value for the first beam.

The experimental dependence (the solid line) between the load-force and the deflection of the three-point bending of this beam is shown in Fig. 13. Additionally, the analytical linear dependence (the broken line) for this beam is presented with a view to compare both methods.

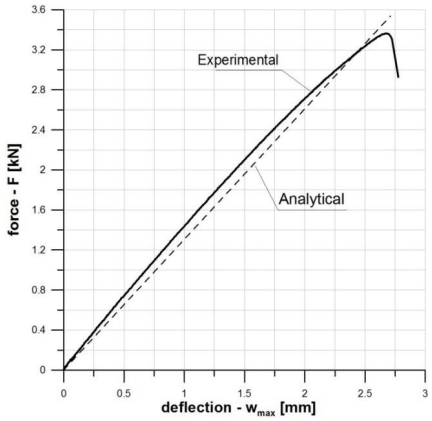

Fig. 13. The experimental and analytical force-deflection curves of the three-point bending (B-2)

4. CONCLUSIONS

The analytical and experimental studies of the three-point bending of seven-layer beam – plate bands led to the following statements:

- the formulated analytical models for both beams (B-1) and (B-2) based on the assumed hypothesis for deformation of the plane cross-sections (Fig. 3 and Fig. 6) is positively verified by the experiments,
- the systems of the equations of equilibrium (2.12) and (2.26) refer to the general bending of seven-layer beam – plate bands, and also the buckling problems,
- analytically calculated stiffness of these two beams provide lower estimations as compared to experimental results (Fig. 10 and Fig. 13),
- the elaborated analytical models for seven-layer beams may be applied to analytical modelling of thin-walled seven-layer structures.

ACKNOWLEDGMENTS

The project was funded by the National Science Centre, allocated on the basis of decision Number DEC-2013/09/B/ST8/00170.

REFERENCES

1. E. Carrera, S. Brischetto, "A survey with numerical assessment of classical and refined theories for the analysis of sandwich plates", Applied Mechanics Reviews 62(1): 010803, 2009.
2. Y-J. Cheon, H-G Kim, "An equivalent plate model for corrugated-core sandwich panels", Journal of Mechanical Science and Technology 29(3): 1217–1223, 2015.
3. S. Kazemahvazi, D. Zenkert, "Corrugated all-composite sandwich structures". Part 1: Modeling. Composite Science and Technology 69(7–8): 913–919, 2009.
4. M. Kotełko, K. Kowal-Michalska, T. Kubiak, z. Kołakowski, R. Grądzki, "Estimation of load-carrying capacity of multi-layered plated structures", Thin-Walled Structures 46: 1003–1010, 2008.
5. J. Lewinski, E. Magnucka-Blandzi, W. Szyc, "Determination of shear modulus of elasticity for thin-walled trapezoidal corrugated cores of seven-layer sandwich plates", Engineering Transactions 63(4): 421–437, 2015.
6. E. Magnucka-Blandzi, K. Magnucki, "Transverse shear modulus of elasticity for thin-walled corrugated cores of sandwich beams, Theoretical study". Journal of Theoretical and Applied Mechanics 52(4): 971–980, 2014.
7. E. Magnucka-Blandzi, K. Magnucki, L. Wittenbeck, "Mathematical modelling of shearing effect for sandwich beams with sinusoidal corrugated cores". Applied Mathematical Modelling 39: 2796–2808, 2015.
8. K. Magnucki, E. Magnucka-Blandzi, L. Wittenbeck, "Elastic bending and buckling of a steel composite beam with corrugated main core and sandwich faces – Theoretical study", Applied Mathematical Modelling, 40: 1276–1286, 2016.
9. P. Paczos, P. Wailewicz, E. Magnucka-Blandzi, "Experimental and numerical investigations of five-layered trapezoidal beams", Composite Structures 145: 129–141, 2016.
10. D.Y. Seong, C.G. Jung, D.Y. Yang, K.J. Moon, D.G. Ahn, "Quasi-isotropic bending responses of metallic sandwich plates with bi-directionally corrugated cores", Materials and Design 31(6): 2804–2812, 2010.
11. J.R. Vinson, "Sandwich structures", Applied Mechanics Reviews, 54(3): 201–214, 2001.
12. M. Piekarczyk, R. Grec: "Application of adhesive bonding in steel and aluminium structures", Archives of Civil Engineering, LVIII(3): 309–329,2012.
13. M. Książek, P. Nowak, S. Kivrak, J. Rosłon, L. Ustinovichius, "Computer-aided decision-making in construction project development", Journal of Civil Engineering and Management, 21(2): 248–259,2015.

LIST OF FIGURES AND TABLES:

TRZY-PUNKTOWE ZGINANIE BELEK SIEDMIO-WARSTWOWYCH – BADANIA TEORETYCZNE I DOŚWIADCZALNE

Słowa kluczowe: rdzenie pofałdowane trapezowo, konstrukcje ortotropowe, pasma płytowe

STRESZCZENIE:

Przedmiotem pracy są dwie stalowe cienkościenne siedmio-warstwowe belki – pasma płytowe z trapezowo pofałdowanymi dwoma rdzeniami okładzin oraz rdzeniem głównym. Obie belki różnią się między sobą kierunkami pofałdowań rdzeni. Belka pierwsza (B-1) (Rys. 1) posiada rdzeń główny pofałdowany jest wzdłuż jej długości, a rdzenie okładzin pofałdowane poprzecznie.

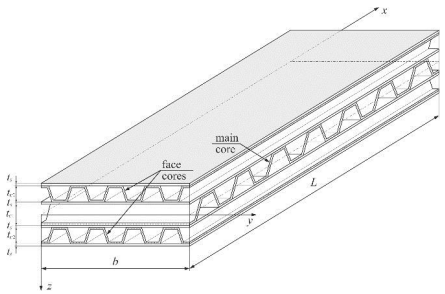

Rys. 1. Scheme of the first beam – plate band (B-1)

Natomiast belka druga (B-2) (Rys. 2) posiada rdzeń główny pofałdowany poprzecznie, a rdzenie okładzin pofałdowane wzdłuż jej długości.

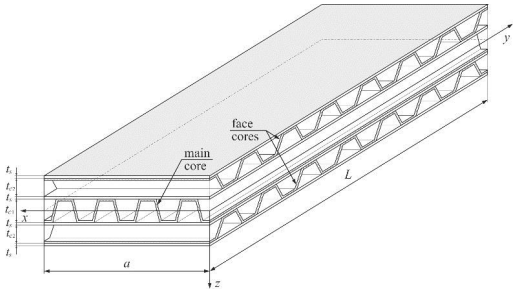

Rys. 2. Scheme of the second beam – plate band (B-2)

Kierunki pofałdowania rdzenia głównego w obu belkach są prostopadłe do kierunków pofałdowań rdzeni okładzin. Rdzeń główny połączony jest z rdzeniami okładzin za pośrednictwem cienkich blach-pasm płaskich. Warstwy zewnętrzne są również cienkimi blachami-pasmami płaskimi. Siedmio-warstwowa struktura tych belek jest więc niejednorodna. Właściwości czterech stalowych cienkich blach-pasm są izotropowe, natomiast właściwości rdzeni postaci pofałdowanych trapezowo cienkich blach są ortotropowe, a ich sztywności na rozciąganie, zginanie i ścinanie

w dwóch kierunkach głównych różnią się znacznie. Zatem, klasyczna teoria Eulera-Bernoulliego zginania belek (hipoteza prostej normalnej) w przypadku przedmiotowych belek – pasm płytowych nie jest poprawna. Opracowano więc dla każdej belki odpowiednią hipotezę deformacji przekroju płaskiego podczas zginania (Rys. 3 oraz Rys. 6). Łatwo zauważyć, że hipotezy te różnią się kształtem „linii łamanej", a powodem są znaczne różnice sztywności w kierunkach pofałdowania rdzeni. Na podstawie tych hipotez sformułowano pola przemieszczeń dla poszczególnych warstw oraz odkształcenia. Uwzględniając następnie prawo Hooke'a, zapisano energię odkształcenia sprężystego dla każdej belki – pasma płytowego oraz pracę obciążenia. Korzystając z zasady stacjonarności całkowitej energii potencjalnej układu wyznaczono równania równowagi dla każdej belki oddzielne w postaci dwóch równań różniczkowych zwyczajnych. Układy tych dwóch równań rozwiązano analitycznie dla przypadku trzy-punktowego zginania i otrzymano zależność ugięcie – obciążenie. Stąd, po prostym przekształceniu wyznaczono wartości sztywności obu belek $k_{B-1}^{(Analyt)}$ oraz $k_{B-2}^{(Analyt)}$ dla przyjętych – zmierzonych wymiarów badanych belek. Następnie, wykonane stalowe belki – pasma płytowe badano doświadczalnie w maszynie wytrzymałościowej. Otrzymano stąd zależności obciążenie – ugięcie $F(w_{\max})$ w postaci wykresów dla każdej belki. W celu porównania wyników otrzymanych z obu metod, naniesiono na wykresy doświadczalne, otrzymane z maszyny wytrzymałościowej, wykresy – linie proste wyznaczone analitycznie (Rys. 10 oraz Rys. 13). Dodatkowo w Tabeli 1 i Tabeli 2 zestawiono dla wybranych wartości ugięć odpowiadające im wartości obciążeń-sił wyznaczonych doświadczalnie i analitycznie. Stwierdzono zgodność otrzymanych wyników z obu metod. Różnice między wartościami sił wyznaczone obiema metodami są mniejsze od 5% dla belki pierwszej oraz mniejsze od 10% dla belki drugiej. Ponadto, rozwiązanie analityczne daje dolne oszacowanie wartości obciążeń. Wynika stąd, że belki rzeczywiste charakteryzuje większa sztywność niż wynikałoby to z rozwiązania analitycznego.

Przedstawione w pracy badania analityczne i doświadczalne zginania siedmio-warstwowych belek o strukturze cienkościennej są badaniami podstawowymi. Szczególne znaczenie mają tu opracowane modele analityczne obu belek. Przegląd literatury wskazuje na aktualność tematyki badawczej dotyczącej wytrzymałości i stateczności konstrukcji warstwowych.